Journal of
MATERIALS RESEARCH

Melt infiltration casting of bulk metallic-glass matrix composites

R. B. Dandliker, R. D. Conner, and W. L. Johnson
W. M. Keck Laboratory of Engineering Materials, Mail Code 138-78, California Institute of Technology, Pasadena, California 91125

(Received 5 May 1997; accepted 5 January 1998)

The authors describe a technique for melt infiltration casting of composites with a metallic-glass matrix. We made rods 5 cm in length and 7 mm in diameter. The samples were reinforced by continuous metal wires, tungsten powder, or silicon carbide particulate preforms. The most easily processed composites were those reinforced with tungsten and carbon steel continuous wire reinforcement. The $Zr_{41.2}Ti_{13.8}Cu_{12.5}Ni_{10.0}Be_{22.5}$ matrix was quenched to a glass after infiltrating the reinforcement. We analyzed the microstructure of the composites by x-ray diffraction and scanning electron microscopy. The measured porosity was less than 3% and the matrix was about 97% amorphous material.

I. INTRODUCTION

Metallic glasses are usually made by rapidly solidifying certain alloys. Most alloys investigated require cooling rates of 10^5 K/s or higher to freeze from the melt to the metastable amorphous state. The high heat transfer rate required limits these metallic glasses to thin samples produced by such techniques as splat quenching or melt spinning.[1,2]

The melt spinning technique has often been used to make amorphous metal matrix composites. Particulate reinforcements have been added to a liquid glass-forming metal alloy and processed with a number of techniques to make composite ribbons.[3–7] Wire and continuous fiber reinforcement of metallic glass ribbons have also been reported, although the best results have yielded a ribbon reinforced with only two continuous wires.[5,8,9]

So-called "bulk" metallic glasses, alloys with critical cooling rates of 10^2 K/s or less, are much more promising as potential matrix materials for composites. These glass-forming alloys are not limited to thin geometries.[10–14] One of the most highly processible of these alloys is $Zr_{41.2}Ti_{13.8}Cu_{12.5}Ni_{10.0}Be_{22.5}$, which has a critical cooling rate of about 1 K/s with no fluxing required.[15] Fully amorphous rods of this alloy of up to 5 cm in diameter have been cast. This amorphous alloy has a yield point of about 1.9 GPa, which is substantially higher than most crystalline metals. In addition, it exhibits approximately 2% elastic strain, again far greater than crystalline materials. These superior mechanical properties and the low critical cooling rate of this bulk metallic glass are the primary reasons for its promise as a new engineering material.[16–19]

This study reports a technique for successfully using the alloy $Zr_{41.2}Ti_{13.8}Cu_{12.5}Ni_{10.0}Be_{22.5}$ as a matrix material for composites. The low critical cooling rate of this alloy allows amorphous metal matrix composites to be made in bulk form.

II. EXPERIMENTAL

In this study we used exclusively the $Zr_{41.2}Ti_{13.8}Cu_{12.5}Ni_{10.0}Be_{22.5}$ (trade name Vitreloy^{TM}1) developed by Peker and Johnson[12] as the matrix material. We first prepared ingots by alloying together the constitutive elements in an induction furnace under a titanium-gettered argon atmosphere. The starting metals were high-purity (99.5% metals basis or better) research grade material.

We fabricated composites with a wide variety of reinforcements using the described technique. Continuous ceramic fibers, such as silicon carbide and carbon, and continuous metal wires, such as tungsten, carbon steel, stainless steel, molybdenum, tantalum, nickel, copper, and titanium, were used as reinforcement. We also made particulate reinforced composites with both loose tungsten particles and sintered silicon carbide (SiC) particulate preforms. The preforms were provided by the Carborundum Company.

We used 254 μm diameter tungsten wire or 254 μm diameter high-carbon (1080) steel music wire as reinforcement in the majority of samples. The tungsten wire was obtained from Thermionics Products Company (North Plainfield, NJ). Both types of wire were straightened and cut into 5 cm lengths. To avoid clumping of wires and to ensure good distribution, we bowed the wires slightly in samples with lower fiber fractions. The tungsten wire was degreased by ultrasonic cleaning in a bath of acetone followed by the same procedure in a bath of ethanol. The steel wire was cleaned in a solution of 50% phosphoric acid and 50% water at room temperature for 3 min. This solution removes the oxide layer while depositing only a thin phosphate layer.

We cast composite specimens in the apparatus shown by the schematic in Fig. 1. The reinforcement material was placed in the sealed end of a 7 mm inner diameter quartz-glass tube. We necked the tube about 1 cm above the reinforcement, and then placed ingots of the matrix

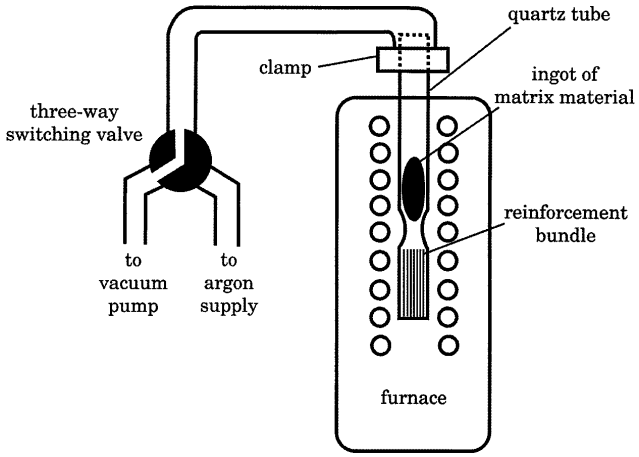

FIG. 1. Schematic diagram of apparatus for casting bulk metallic-glass matrix composites.

material in the tube above the neck. The constriction minimizes premature contact and thus excessive reaction between the melt and the reinforcement. We then connected the open end of the quartz tube to a three-way switching valve; the tube could thus be evacuated with a roughing pump or pressurized with argon. Prior to heating, we evacuated the tube and then flushed it with argon gas. This cycle was repeated several times to remove any residual oxygen. The tube was left under vacuum on the last cycle to minimize trapped gas in the composite sample to be formed. An additional processing step was required for casting the steel wire composites. The wires were held at 973 K for 2 h under vacuum to remove any hydrogen absorbed by the steel during the acid etch.

The sample tube was heated in a resistive tube furnace with temperature feedback control. The initial heating stage was at 1228 K $\pm$ 20 K, well above the liquidus temperature (993 K)[12] of the glass-forming alloy. This initial heating stage was found useful in dissolving residual oxides and other impurity phases which degrade the glass forming ability of the alloy.[20] The variation in temperature comes primarily from the temperature profile in the furnace. The sample was held at this temperature for 15 min. The temperature was then lowered to 1078 K $\pm$ 5 K and allowed to stabilize. When the furnace reached this target temperature, a positive pressure of 207 kPa argon was applied above the melt. These conditions were held for 30 min to allow infiltration of the molten matrix material into the reinforcement. Then the sample was quickly removed from the furnace and quenched in brine (8 wt. % $NaCl/H_2O$ solution). To improve the mechanical properties of the steel, some of the steel wire reinforced samples were tempered at 588 K for 2 h following infiltration and quenching.

The composite samples were sliced normal to the fiber orientation. We obtained x-ray diffraction patterns of the slices using an Inel diffractometer with a position sensitive detector and Co K_α radiation (wavelength = 0.1790 nm). The cut surface was then polished and analyzed with scanning electron microscopy (SEM).

Porosity was estimated by two methods. The first finds the apparent porosity by analysis of a micrograph of a cross-sectioned sample. The bulk sample porosity can then be extrapolated by assuming homogeneity throughout the sample. This technique has been used for other materials as described in an ASTM standard.[21]

The second method of determining porosity combines analysis of the cross section with Archimedes' principle. As a consequence of the processing procedure, the volume fraction of reinforcement cannot be inferred from the relative amounts of the starting materials. There is a substantial reaction layer between the as-processed composite and the quartz tube, as well as a layer of quartz which strongly adheres to this reaction layer. The quartz layer and the reaction layer must be ground off mechanically; unavoidably, some of the reinforcement and matrix is removed as well. As a result, we cannot make a precise determination of the volume fractions from the amounts of the starting materials.

The volume fraction of wires was computed by analyzing a backscatter SEM micrograph of the polished cross section of the sample. The relative area covered by the matrix and continuous reinforcement then gives the volume fraction of wires directly. Archimedes' principle was used to find the overall density of the sample. Then, having both the density of the sample and the volume fraction, we determined the porosity.

III. RESULTS

The quality of the composite samples produced by this technique varied with the reinforcement. At least one sample with each type of reinforcement listed in the previous section was made. The samples were judged on the extent of infiltration and the percentage of matrix which was amorphous. On this basis, tungsten and carbon steel continuous wires were chosen for more extensive study; samples of each with nominal reinforcement volume fractions of 20, 40, 60, and 80% were made.

We measured the porosity of two samples: one with nominally 60 vol % tungsten wire reinforcement and the other 80 vol %. Upon evaluation of SEM micrographs of polished cross sections, the apparent porosity of the composites was found to be less than 1%. By calculating the volume fraction and using Archimedes' principle as described in the previous section, we determined a porosity of 3% $\pm$ 2%.

The quality of the tungsten-reinforced composites was very consistent; more complications arose in making the steel wire reinforced composites. We found that gases

were released from the steel wires during processing. The samples with nominal 20 and 40 vol % steel wire were made before the problem was found, and thus without the bakeout procedure. To avoid trapped gas porosity and hydrogen embrittlement of the steel, the bake out procedure was added prior to processing the composite samples in the 60 and 80 vol % steel samples.

Figure 2 shows typical x-ray diffraction patterns of two cross-sectioned composite samples. The x-axis values of the patterns have been converted from two theta values to interplanar spacings using Bragg's Law. One pattern is of a composite reinforced with 20 vol % steel music wire, and another is of a sample reinforced with 20 vol % tungsten wire. For comparison, the pattern from an unreinforced sample of the matrix material is included. The unreinforced matrix pattern shows the broad diffraction peaks typical of a fully amorphous structure. The same broad peaks are also visible in these lower reinforcement volume fraction samples, but the matrix pattern is obscured for higher fractions because of the large intensity difference between the Bragg peaks of the reinforcement and the broad amorphous bands.

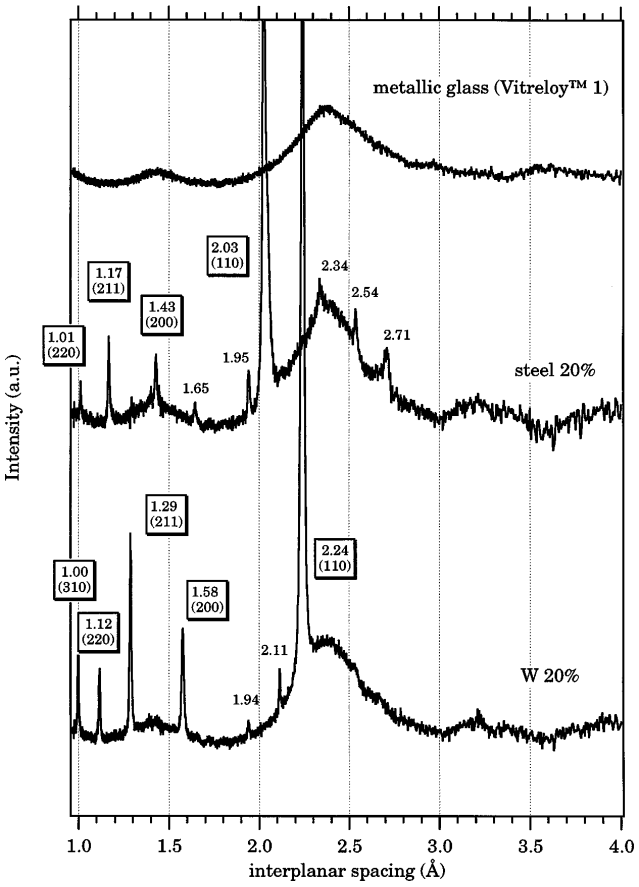

FIG. 2. X-ray diffraction pattern of cross-sectioned uniaxially reinforced bulk metallic-glass matrix composites. Co radiation (λ = 1.7902 Å) was used. Percentages shown are nominal volume fractions of reinforcement, and the balance is the metallic glass matrix.

The first four bcc reflections for iron are visible in the steel reinforced samples, and the first five bcc peaks of tungsten in the tungsten composites. The peaks from the reinforcement material are labeled in boxes with the corresponding interplanar spacing and the index of the reflection. There are also some additional small crystalline peaks visible in the patterns of samples with low reinforcement fractions. The number beside each small peak corresponds to its interplanar spacing.

The peaks at 1.65 Å, 2.34 Å, and 2.70 Å in the steel reinforced sample correspond to the three high intensity peaks from ZrC. We expect carbon in the steel to react with elements in the molten matrix and form carbides at the reinforcement/matrix interface. This explains the presence of ZrC peaks in the pattern. In addition, from examining the splitting in the (110) peak of the steel diffraction pattern, we can estimate the final carbon content to be about 0.27 wt. %. The initial carbon content was 0.80 wt. %, so this again suggests the diffusion of carbon from the wires could lead to carbide formation at the interface.

SEM micrographs of an 80 vol % tungsten-wire reinforced composite are shown in Figs. 3 and 4. Figure 3 is an overview of the structure, and Fig. 4 is a higher magnification image of the interfacial region. Most of the matrix is amorphous, but there are dark-contrast crystals visible in the matrix near the matrix-wire interface. In the tungsten and steel wire composites we found that 1 vol % to 5 vol % of the matrix was crystalline, depending on the sample. Figure 5 shows an SEM micrograph of a steel wire reinforced composite sample. Two wires are partially visible in the upper right and lower left portions of the image. Crystals are clearly visible in the matrix on the interface with the wires. Nevertheless, the total amount of crystallized matrix remains small. The very

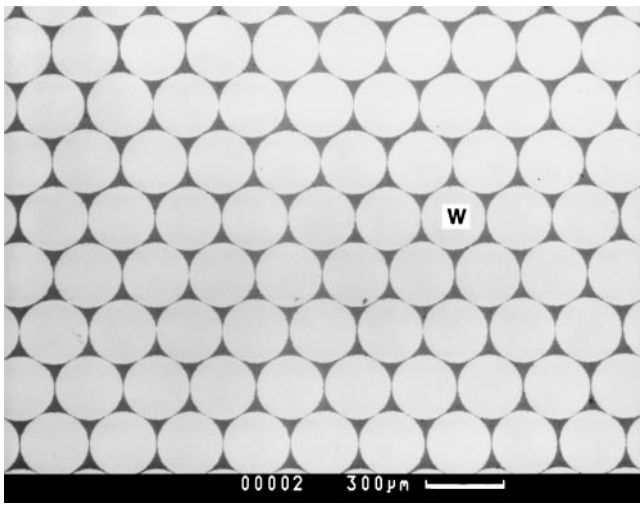

FIG. 3. SEM micrograph in backscatter mode of 80 vol % W wire/bulk metallic-glass matrix composite. Sample is polished slice cut normal to uniaxial reinforcement.

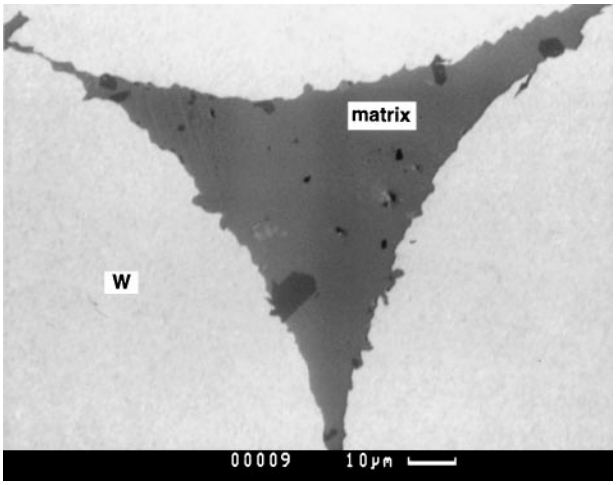

FIG. 4. SEM micrograph in backscatter mode. Same sample and preparation as Fig. 3. Lighter regions are W wire; darker region is matrix. Very dark regions are small crystallized portions of the matrix.

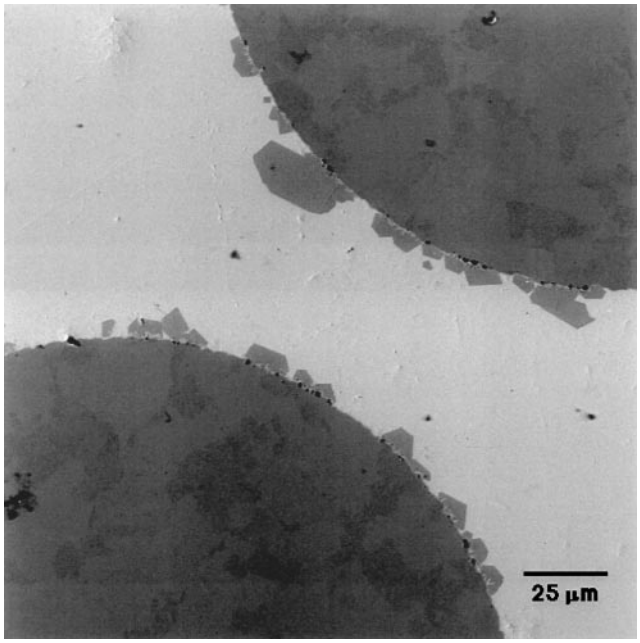

FIG. 5. SEM micrograph of 60 vol% steel-wire-reinforced bulk metallic-glass matrix composite. Image from backscatter detector. Wires appear dark, and matrix appears light. Small darker regions of crystallized matrix are visible near wire reinforcement.

small dark regions directly on the wire/matrix interface are most likely carbides resulting from the reaction between elements in the matrix and carbon from the steel.

Figure 6 is a stress-strain curve for samples produced by these techniques. The samples were cylinders 6.35 mm in diameter, and approximately 12 mm long. The samples were tested in compression until failure. The figure shows, from left to right, a sample of unreinforced metallic glass, a sample with 60 vol% 1080 steel wire reinforcement, and a sample with 60 vol% tungsten

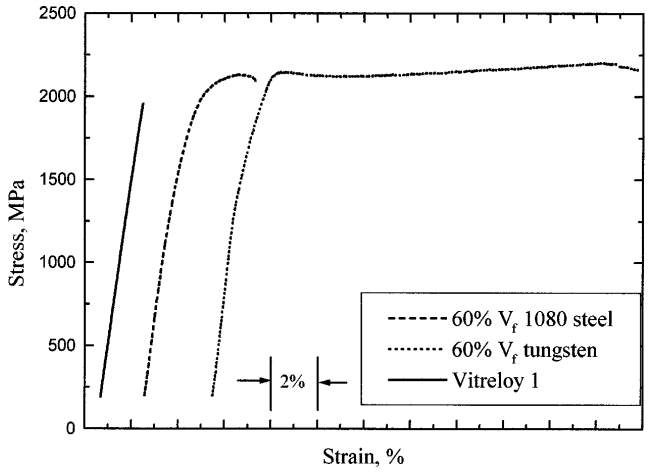

FIG. 6. Stress-strain curve for compression testing of metallic glass composites. From left to right: unreinforced metallic glass (Vitreloy^{TM} 1 composition), metallic glass reinforced with 60 vol% continuous steel wire, and metallic glass reinforced with 60 vol% continuous tungsten wire.

wire reinforcement. Note that the unreinforced metallic glass is elastic up to 1900 MPa, and shows no significant plastic deformation. The composite reinforced with steel wire has over 2% plastic strain and slightly improved ultimate strength. The composite sample reinforced with tungsten wire also has an increased ultimate strength, in addition to nearly 16% plastic strain before failure.

Figure 7 is an optical micrograph of a porous preform infiltrated with metallic glass. The preform is made of silicon carbide particles sintered to 60% density. Inspection of the micrograph shows full infiltration of the preform by the metallic glass and apparently a

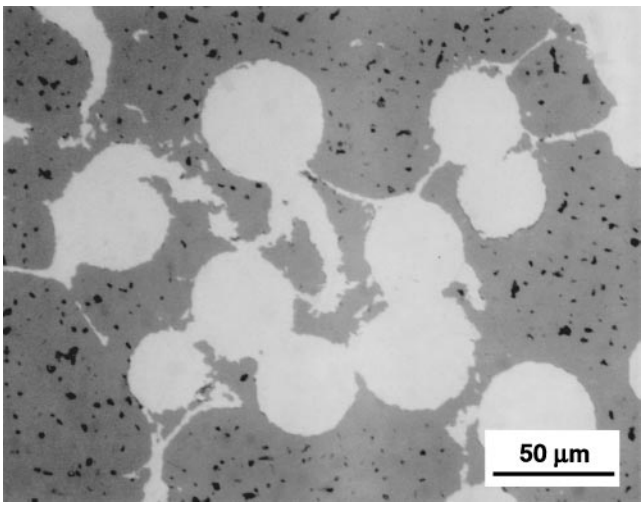

FIG. 7. Optical micrograph of SiC preform infiltrated with bulk metallic glass. Dark regions are SiC, and light regions are amorphous metal. Notice the infiltration of the melt into very fine features of the preform and the absence of crystallized matrix material.

fully amorphous matrix. X-ray diffraction of this sample showed crystalline peaks only from silicon carbide.

IV. DISCUSSION

As mentioned previously, the choice of matrix composition and reinforcement materials was largely motivated by ease of processing. To take advantage of the mechanical properties of the metallic glass in the composite, it is important to avoid crystallization of brittle intermetallics.[16] Clearly, for quenching a sample from the melt, a low critical cooling rate is advantageous and allows larger samples to be easily processed and fabricated. $Zr_{41.2}Ti_{13.8}Cu_{12.5}Ni_{10.0}Be_{22.5}$ has one of the lowest reported critical cooling rates of any metallic glass forming alloy. In addition, the low liquidus temperature of the alloy allows processing of the molten alloy at a relatively low temperature, and, accordingly, results in a minimal reaction between the matrix and reinforcement.

The extremely high melting point of tungsten (3680 K) is consistent with both a small thermal effect on the microstructure of the wire during processing and limited reactivity with the melt. Although the microstructure of steel is not as stable at the processing temperatures, the glass is tolerant of small additions of iron,[22] making steel a good reinforcement material as well.

The crystals in the matrix are most likely due to impurities on the surface of the reinforcement. Preliminary analysis shows that dissolved reinforcement material is not a significant constituent of the crystals; however, Figs. 4 and 5 clearly show more crystallization near the matrix-reinforcement interface. However, in the reinforced samples, some crystals appeared in the matrix far away from any reinforcement material. No crystals were present in similarly processed unreinforced samples. The larger amount of crystallized matrix material in the steel wire reinforced samples is most likely due to larger amounts of oxides on the steel than on the tungsten. Identification of the crystalline phases present as well as results of mechanical tests will be addressed in later publications.

Nevertheless, addition of reinforcements to a bulk metallic glass can allow samples to be made larger than with the glass alone. The amorphous matrix material has a thermal conductivity of about 0.035 W cm^{-1} K^{-1} at room temperature. We would expect a somewhat lower thermal conductivity for the undercooled melt, which is the material of interest in determining critical cooling rates. Tungsten and carbon steel have thermal conductivities of 1.74 W cm^{-1} K^{-1} and 1.0 W cm^{-1} K^{-1}, respectively,[23] and remain solid during the processing. The addition of higher thermally conductive materials in the composite allows heat to be removed from the composite more efficiently than in the unreinforced amorphous alloy, thus allowing the critical cooling rate to be reached in larger samples.

During the initial stage of processing, prior to infiltration, the metallic glass is preheated to the minimum temperature required to remelt any residual crystalline particles present in the starting ingots. Lin *et al.* found in another bulk glass-former that preheating a few hundred degrees above the melting temperature is necessary to achieve maximum undercooling.[20] The conclusion from that study is that crystallization of the melt is controlled by nucleation of oxide particles; the preheat must exceed the liquidus temperature of the oxides to get maximum undercooling. We expect a similar phenomenon in the Zr–Ti–Cu–Ni–Be system. This study provided the motivation for the initial preheating step discussed earlier.

Under the given processing conditions, unreinforced metallic glass samples are fully amorphous under x-ray diffraction analysis. At higher temperatures, the viscosity of the melt drops and the likelihood of exposing the reinforcement to the melt prematurely increases. At the temperature of the preheat step, we found significantly more reaction between the reinforcement and matrix. In addition, even if the neck in the quartz tube succeeds in preventing contact between the melt and the reinforcement, there is reaction between the melt and the quartz. Titanium, zirconium, and beryllium all form very stable oxides; all three are more thermodynamically stable than silicon dioxide per mole of oxygen. Thus, we expect the quartz to be reduced by contact with the melt. This reaction is obvious in the final sample and is responsible for the observed interlayer between the composite and the quartz. This is unavoidable to some extent with this technique, but because we suspect that oxygen is detrimental to the glass-forming ability of this alloy, we try to minimize this silica reduction reaction.

We chose the processing conditions to minimize the total reaction between the reinforcement and the matrix. In some cases, it is possible that some reaction is desirable for optimal interfacial characteristics. For insufficient interfacial reactions, reaction time can simply be extended. Far more common is the problem of excess reaction between matrix and reinforcement.

Conditions for the final stage of processing were chosen to allow sufficient time for full infiltration of the reinforcement by the melt with minimal reaction. Because of its higher viscosity, the glass-forming alloy takes longer to infiltrate the reinforcement than conventional metal matrix materials do. At the temperature of this processing step, the viscosity of the molten alloy is about 4 Pa-s.[24] By comparison, aluminum at its melting point is about 1 mPa-s.[23] Lower viscosities at higher temperatures would allow shorter infiltration times, but with increased reaction between the matrix and reinforcement. We found that there was more reaction

between matrix and reinforcement at higher temperatures, despite shorter processing times.

The mechanical testing showed that the addition of reinforcement can significantly improve certain mechanical properties in the composite over those of the unreinforced metallic glass. For instance, the strain-to-failure in the composite reinforced with 60 vol % tungsten was nearly 16% at a strength higher than could be sustained in the unreinforced metallic glass. Further mechanical testing will be presented in later papers.

Although the two samples measured have low porosity, we suspect this number may not be representative of all samples, particularly those of lower volume fractions. More samples need to be measured to obtain a better statistical sampling.

V. CONCLUSIONS

Composites with a bulk metallic-glass matrix can successfully be made by slow melt infiltration of the reinforcement. Given the right processing conditions, very little reaction occurs between the matrix and reinforcement, and the matrix freezes to an amorphous structure. Many reinforcement materials and geometries can be used successfully. The most easily processed composites were reinforced with uniaxial tungsten and steel wires, and silicon carbide particulate preforms. The matrix material used was $Zr_{41.2}Ti_{13.8}Cu_{12.5}Ni_{10.0}Be_{22.5}$, but this technique should be applicable with other bulk metallic glass alloys.

ACKNOWLEDGMENTS

This report is based upon work supported in part by the U.S. Army Research Office under Grant No. DAAH04-95-1-0233. We would like to thank M. Tenhover and H. Choi-Yim for useful discussions. In addition, we would like to thank Dr. Tenhover and Carborundum Corporation for supplying silicon carbide fibers and preforms.

REFERENCES

1. W. Klement IV, R. H. Willens, and P. Duwez, Nature (London) **187**, 869 (1960).
2. H. H. Liebermann, in *Amorphous Metallic Alloys,* edited by F. E. Luborsky (Butterworths, London, 1983), pp. 26–41.
3. H. Kimura, B. Cunningham, and D. G. Ast, in *Proc. 4th Int. Conf. on Rapidly Quenched Metals,* edited by T. Masumoto and K. Suzuki (Jpn. Institute of Metals, Sendai, Japan, 1982), pp. 1385–1388.
4. P. G. Zielinski and D. G. Ast, J. Mater. Sci. Lett. **2**, 495 (1983).
5. P. G. Zielinski and D. G. Ast, in *Rapidly Solidified Metastable Materials,* edited by B. H. Kear and B. C. Giessen (Mater. Res. Soc. Symp. Proc. **28**, Elsevier, New York, 1984), pp. 189–195.
6. D. G. Ast, U.S. Patent 4,523,625 (1985).
7. M. Narasimhan, U.S. Patent 4,330,027 (1982).
8. J. F. Williford and J. P. Pilger, U.S. Patent 3,776,297 (1973).
9. G. Nussbaum and D. G. Ast, J. Mater. Sci. **22**, 23 (1987).
10. H. S. Chen and D. Turnbull, Acta Metall. **17**, 1021 (1969).
11. A. J. Drehman, A. L. Greer, and D. Turnbull, Appl. Phys. Lett. **41**, 716 (1982).
12. A. Peker and W. L. Johnson, Appl. Phys. Lett. **63**, 2342 (1993).
13. T. Zhang, A. Inoue, and T. Masumoto, Mater. Trans. JIM **32**, 1005 (1991).
14. X. Lin and W. L. Johnson, J. Appl. Phys. **78**, 6514 (1995).
15. Y. J. Kim, R. Busch, W. L. Johnson, A. J. Rulison, and W. K. Rhim, Appl. Phys. Lett. **68**, 1057 (1996).
16. W. L. Johnson, in *Materials Science Forum Proc. ISMANAM-95,* edited by R. Schultz (Transtec, Switzerland, 1996), pp. 35–50.
17. W. L. Johnson, Curr. Opinion in Solid State Mater. Sci. **1**, 383 (1996).
18. H. A. Bruck, T. Christman, A. J. Rosakis, and W. L. Johnson, Scripta Metall. Mater. **30**, 429 (1993).
19. H. A. Bruck, A. J. Rosakis, and W. L. Johnson, J. Mater. Res. **11**, 503 (1996).
20. X. Lin and W. L. Johnson, subm. Mater. Trans. JIM (1997).
21. *Annual Book of ASTM Standards,* Vol. 02.05 (ASTM, Philadelphia, PA, 1991).
22. A. Peker and W. L. Johnson, U.S. Patent 5,288,344 (1994).
23. *Handbook of Chemistry and Physics* (CRC Press, Boca Raton, FL, 1991).
24. R. Busch, A. Masuhr, E. Bakke, and W. L. Johnson, in *MRS 1996 Fall Symp. on Glasses and Glass Formers* (1997).